Veterinary Microbiology 239 (2019) 108455

Contents lists available at ScienceDirect

Veterinary Microbiology

journal homepage: www.elsevier.com/locate/vetmic

Mortalin restricts porcine epidemic diarrhea virus entry by downregulating clathrin-mediated endocytosis

Baochao Fan[a,b,c,d], Lin Zhu[a,b], Xinjian Chang[a,b], Jinzhu Zhou[a,b,c], Rongli Guo[a,b], Yongxiang Zhao[a,b], Danyi Shi[a,b,c,e], Beibei Niu[a,b,f], Jun Gu[a,g], Zhengyu Yu[a,b,c], Tao Song[e], Chuping Luo[d], Zengjun Ma[e], Juan Bai[f], Bin Zhou[f], Siyuan Ding[h], Kongwang He[a,b,c,*], Bin Li[a,b,c,f,g,*]

[a] Institute of Veterinary Medicine, Jiangsu Academy of Agricultural Sciences, Key Laboratory of Veterinary Biological Engineering and Technology, Ministry of Agriculture, Nanjing, Jiangsu 210014, China
[b] Jiangsu Co-innovation Center for Prevention and Control of Important Animal Infectious Diseases and Zoonoses, Yangzhou University, Yangzhou, Jiangsu 225000, China
[c] Jiangsu Key Laboratory for Food Quality and Safety-State Key Laboratory Cultivation Base of Ministry of Science and Technology, Nanjing 210014, China
[d] Jiangsu Provincial Key Construction Laboratory of Probiotics Preparation, Huaiyin institute of technology, Huaian 223003, China
[e] College of Animal Science and Technology, Hebei Normal University of Science and Technology, Qinhuangdao 066004, China
[f] College of Veterinary Medicine, Nanjing Agricultural University, No.1 Wei-gang, Nanjing 210095, China
[g] School of Food and Biological Engineering, Jiangsu University, Zhenjiang 212013, China
[h] Department of Molecular Microbiology, Washington University in St. Louis, MO 63110, United States

ARTICLE INFO

Keywords:
Mortalin
PEDV
CLTC
Clathrin-mediated endocytosis

ABSTRACT

Clathrin-mediated endocytosis is a mechanism used for the invasion of cells by a variety of viruses. Mortalin protein is involved in a variety of cellular functions and plays a role in viral infection. In this study, we found that mortalin significantly inhibited the replication of porcine epidemic diarrhea virus (PEDV) through restricting virus entry. Mechanistically, a biochemical interaction between the carboxyl terminus of mortalin and clathrin heavy chain (CLTC) was been found, and mortalin could induce CLTC degradation through the proteasomal pathway, thereby inhibiting the clathrin-mediated endocytosis of PEDV into host cells. In addition, artificial changes in mortalin expression affected the cell entry of transferrin, further confirming the above results. Finally, we confirmed that this host-mounted antiviral mechanism was broadly applicable to other viruses, such as vesicular stomatitis virus (VSV), rotavirus (RV), and transmissible gastroenteritis virus (TGEV), which use the same clathrin-mediated endocytic to entry. These results reveal a new function of mortalin in inhibiting endocytosis, and provide a novel strategy for treating PEDV infections.

1. Introduction

Porcine epidemic diarrhea (PED) is characterized by severe watery diarrhea, leading to dehydration and high mortality among piglets. This disease is caused by porcine epidemic diarrhea virus (PEDV), which belongs to the family *Coronaviridae*, genus *Alphacoronavirus*, and has an envelope surrounding its single-stranded positive-sense RNA genome (Pensaert and de Bouck, 1978). The genome of PEDV is approximately 28 kb in length, containing an 5´untranslated region (UTR), a 3´UTR with a polyadenylated tail, and at least seven open reading frames (ORFs), arranged as follows: 5´UTR - ORF1a/1b - spike (S) - open reading frame 3 (ORF3) - envelope (E) - membrane (M) - nucleocapsid (N) - 3´UTR (Bridgen et al., 1998).

PED was first identified in the United Kingdom and Belgium in the early 1970s (Pensaert and de Bouck, 1978), with reports of its occurrence in China as early as the 1980s (Xuan et al., 1984). Since October 2010, serious disease epidemics have been observed in China with new PEDV variants(Li et al., 2012; Sun et al., 2012). This disease has rapidly spread to the US, as well as to other countries in South America, Asia, and Europe, with considerable economic losses to the global pig industry(Lin et al., 2016). To study the pathogenic mechanism and immune regulation between PEDV and the host, several proteomic analyses have been reported using virus-infected Vero cells (Xiaozhen et al., 2016; Zeng et al., 2015), porcine intestinal epithelial IPEC-J2 cells (Lin et al., 2017), and porcine jejunum tissues (Li et al., 2016). Generally, the interactions exist in many functions between PEDV and

* Corresponding authors at: Institute of Veterinary Medicine, Jiangsu Academy of Agricultural Sciences, 50 Zhong-ling Street, Nanjing 210014, China.
E-mail addresses: kongwanghe@126.com (K. He), nana@126.com (B. Li).

https://doi.org/10.1016/j.vetmic.2019.108455
Received 21 August 2019; Received in revised form 1 October 2019; Accepted 7 October 2019

host, such as transcriptional patterns, the cell cycle, the cytoskeleton, apoptosis pathways, the immune system, stress responses, and inflammation.

Mortalin, also known as mtHsp70/PBP74/Grp75/HSPA9, is a member of the heat-shock protein (Hsp)70 family. Among all of the HSP70 family genes, mortalin, which is heat-uninducible, plays a unique role in the upkeep of mitochondria, maintaining mitochondrial homeostasis by acting as an essential component of the translocational machinery in the inner mitochondrial membrane complex (Mokranjac and Neupert, 2009). As a molecular chaperone, mortalin interacts with other proteins and functions in regulating the cellular stress response, cell proliferation, and apoptosis (Flachbartova and Kovacech, 2013). Recently, it was shown that mortalin is involved in tumor processes through interaction with wild-type p53(Wadhwa et al., 2002). Furthermore, mortalin appears to play multiple roles in membrane-mediated macromolecular transport, endocytosis and exocytosis (Flachbartova and Kovacech, 2013).

Clathrin is a trimer of heavy-chain subunits (CLTC), each binding a single light chain subunit (Kirchhausen et al., 2014). Clathrin-mediated endocytosis is a well-characterized endocytic pathway, and it is also a main route via which several viruses enter cells, including PEDV (Park et al., 2014). In this study, we found that the mortalin inhibited the replication of PEDV at the stage of virus entry. Subsequently, we found a biochemical interaction between the carboxyl terminus of mortalin and CLTC, and discovered that mortalin induced CLTC degradation through the proteasomal pathway, thereby inhibiting the clathrin-mediated endocytosis of PEDV into host cells. These findings provide insight into how the host defends against virus entry and potentially provide a novel strategy for treating virus infections.

2. Methods

2.1. Viruses and cells

Cell lines Vero-81 (ATCC No. CCL-81), MA104, HeLa, IPEC-J2, Marc-145 and porcine alveolar macrophages 3D4/21, which were stored in our laboratory, were cultured in Dulbecco's Modified Eagle's Medium (DMEM; Thermo Fisher Scientific, CA, USA) supplemented with antibiotics (100 units/mL of penicillin and 100 mg/mL of streptomycin), and 5% heat-inactivated fetal bovine serum (FBS; Thermo). The classical PEDV strain JS2008 (GenBank accession number: KC109141) and a highly pathogenic variant strain AH2012/12 (GenBank accession number: KU646831) were isolated from pig farms in China (Fan et al., 2016; Li et al., 2013). Rotavirus (RV), and transmissible gastroenteritis virus (TGEV), vesicular stomatitis virus (VSV) and classical swine fever virus (CSFV) were stored in our laboratory, and the 50% tissue culture infection dose ($TCID_{50}$) of these viruses were determined by titration in adapted cells and stored at -80 °C.

2.2. Construction of expression plasmids

Total RNA was extracted from Vero or IPEC-J2 cells using a QIAprep RNA mini kit (Qiagen, Hilden, Germany) and cDNA synthesis was performed with SuperScript III Reverse Transcriptase (Thermo). The full-length mortalin and CLTC, and their truncations, were amplified using Phanta® Max High fidelity amplification enzyme (Vazyme, Nanjing, China) with the specified sets of primers (Table s1). The modified vector pLVX-N1 without the cherry tag was obtained using a recombinant cloning method with primers LVX-qCH-F and LVX-qCH-R (Table s1). And amplicons were cloned into pLVX-N1 using the recombinant cloning kit ClonExpress® II (Vazyme). The determined nucleotide sequences of monkey-origin mortalin, swine-origin mortalin (pMor), and CLTC were found in the GenBank database under accession numbers XM_015140986.1, XM_005661695.3, and XM_023204648.1, respectively. The recombinant vectors of mortalin and its truncations (pLVX-Mor, pLVX-Mor-NBD, and pLVX-Mor-SBD) were expressed including a His tag at the carboxyl terminus, and CLTC and its truncations (pLVX-CLTC, pLVX-CLTC(1–494), pLVX-CLTC(1–1073), and pLVX-CLTC-Hub) were expressed including a HA tag at the carboxyl terminus.

2.3. The effects of mortalin on PEDV replication

20nM mortalin siRNA (siMor-1, siMor-2 or siMor-3) or negative control siRNA (siNC) (Ribobio, Guangzhou, China), and 1 μg of expressed vectors of pLVX-N1, pLVX-Mor or mortalin truncations were transfected into Vero cells using Lipofectamine 3000 transfection reagent according to the manufacturer's recommendations (Thermo), respectively. After 24 h, all cells were infected with PEDV JS2008 or AH2012/12 at a multiplicity of infection (MOI) 0.1 with trypsin (5 μg/ml), which was needed in to virus entry cells (Fan et al., 2016). At 24 h post infection (hpi), the cells were analyzed the expression levels of mortalin and PEDV-N by western blotting with mouse anti-mortalin monoclonal antibody (Thermo) and mouse anti-PEDV-N monoclonal antibody (obtained in our lab), and PEDV yields in the supernatant were titrated by the $TCID_{50}$.

2.4. Assays to determine the effects of mortalin on the key stages of virus replication

This experiment was assayed according to the previous report with little modification (Duan et al., 2015). Briefly, Vero cells at 80% confluence were transfected with 20 nM of siMor-1 or siNC. After 24 h, the plates were pre-chilled at 4 °C for 30 min. Then the cells were incubated with PEDV at a MOI of 5 for 1 h at 4 °C to allow virus attachment without internalization. The cells were washed with ice-cold PBS three times so that unbound viruses were removed. Then a part of the cells were used to extract the total RNA to evaluate the effect of mortalin on PEDV adsorption. The remaining cells were cultured in fresh serum-free DMEM with 5 μg/ml trypsin and subsequently shifted to 37 °C to allow virus internalization. After 1 h, the cells were washed with citrate buffer solution (pH = 3) to remove the non-internalized virions, followed by three washes with ice-cold PBS. The total RNA of infected cells was extracted and used to perform qRT-PCR to evaluate the effects of mortalin on PEDV internalization.

To determine whether mortalin inhibits PEDV at the replication and release steps, Vero cells were incubated with PEDV at a MOI of 0.1 with 5 μg/ml trypsin, and cultured in 37 °C for 2 h, then the cell-free virus particles were removed and the cells were transfected with 20 nM siMor-1 or siNC. At 12 h, 24 h and 36 h, the infected cells were analyzed by western blotting and qRT-PCR. PEDV yields in the supernatant were titrated by the $TCID_{50}$.

To test the effects of mortalin on the entry of other viruses mediated by clathrin, pLVX-Mor was transfected into HeLa and MA104 cells; pLVX-pMor was transfected into IPEC-J2 and 3D4/21 cells; and pLVX-N1 was used as a control. The siRNAs of human- or monkey-origin mortalin were transfected into HeLa and MA104 cells; the mixture of siRNAs of swine-origin mortalin (si-pMor) were transfected into IPEC-J2 and 3D4/21 cells; and siNC was used as a control. After 24 h, HeLa, MA104, IPEC-J2 and 3D4/21 cells were pre-chilled at 4 °C for 30 min, and infected with VSV, RV, TGEV and CSFV at a MOI of 5 for 1 h at 4 °C, respectively. After 1 h, the cells were washed, and were then shifted to 37 °C for another 1 h. And the total RNA of the infected cells was extracted and used to perform qRT-PCR to evaluate the effects of mortalin on virus internalization.

2.5. Mass spectrometry analysis and immunoprecipitation assay

Vero cells were infected with AH2012/12 at a MOI of 0.1 with trypsin. After 24 h, the non-infected and virus-infected cells were washed three times with cold PBS. Cells were then lysed in protein extraction reagent for 30 min on ice, followed by centrifugation at

10,000 × g for 10 min at 4 °C to remove cell debris. Cell extracts were incubated with mouse anti-mortalin monoclonal antibody (Thermo) for 12 h at 4 °C, then A/G-agarose beads (Beyotime, Shanghai, China) were added. After 4 h incubation, the beads were collected by centrifugation at 2500 × g for 5 min and washed five times with cold PBS. The beads were boiled in 2 × SDS loading buffer to elute bound protein and then mass spectrometry analysis was performed by Genecreat (Wuhan, China).

To assay the interaction between complete or truncated mortalin and CLTC, Vero cells were transfected with pLVX-Mor or pLVX-Mor-SBD and pLVX-CLTC or pLVX-CLTC-Hub, respectively. After 24 h, the cells were lysed as described above. Cell lysates were then incubated with rabbit anti-HA (Santa Cruz) or mouse anti-His (Beyotime) antibodies, and the elution samples were analyzed with mouse anti-His or rabbit anti-HA antibodies.

2.6. The assay of degradation pathway

This experiment was assayed according to the previous report with little modification (Hiroshi et al., 2015). Briefly, Vero cells cultured with 80% confluence. Then the proteasome inhibitor lactacystin (5 μM) or the lysosomal inhibitors pepstatin A/E64D (pepstatin A: 10 μg/ml; E64D: 10 μg/ml) were added to the cell cultures. Control cells were incubated with dimethyl sulfoxide (DMSO). After 1 h treatment, the cells were transfected with pLVX-Mor and pLVX-N1 or siMor-1 and siNC for 24 h, respectively. Then the expression levels of CLTC and mortalin were detected, and relative expression levels of CLTC according to the grayscale of β-actin were assayed.

2.7. Assay of the effect of mortalin on clathrin-mediated endocytosis

This experiment was assayed according to the previous report with little modification (Zhang et al., 2018). Briefly, Vero cells plated onto a cover glass in a 24-well plate were transfected with mortalin siRNA and siNC or pLVX-Mor and pLVX-N1, respectively. After 24 h, the cells were pre-chilled at 4 °C for 30 min, and incubated with 25 μg/ml of Alexa Fluor 555-transferrin (Tf; Thermo) or 20 μg/ml of Alexa Fluor 555-cholera toxin subunit B (CT-B; Thermo) for 30 min at 4 °C to synchronize entry, and were then shifted to 37 °C for another 15 min. Then the cells were fixed in 2% PFA and analyzed using a Zeiss LSM 710 scanning confocal microscope.

2.8. The assay of mortalin and clathrin-mediated endocytosis on PEDV entry

Vero or IPEC-J2 cells with 80% confluence were transfected with siMor-1 or siNC for 24 h, respectively. The inhibitor of clathrin-mediated endocytosis: CPZ, was added with concentration 10 μg/ml for 30 min (Park et al., 2014). Control cells were incubated with DMSO. Then the cells were pre-chilled at 4 °C for 30 min, and incubated with AH2012/12 (MOI = 5) for 1 h at 4 °C with trypsin, and were then shifted to 37 °C for another 1 h. The protein levels of mortalin and CLTC and the relative quantifications of PEDV entry numbers in the infected cells were assayed.

2.9. Quantitative reverse transcriptase PCR (qRT-PCR)

Total RNA from the cells was extracted using a total RNA kit (Omega, Guangzhou, China), and the RNA was converted to cDNA using the HiScriptII Q RT SuperMix (+gDNA wiper) (Vazyme) according to the manufacturer's instructions. The specific primers of mortalin, PEDV N, and the other viruses were shown in Table s1. Standard curve analysis was performed for relative quantification. The transcript levels of target genes were relatively quantified using the $2^{-\Delta\Delta CT}$ method. The GAPDH gene served as an internal reference. The relative amount of target gene mRNA was normalized to that of GAPDH mRNA in the same sample.

2.10. Immunofluorescence

Vero cells plated onto a cover glass in a 24-well plate were transfected with pLVX-Mor, pLVX-Mor-NBD or pLVX-Mor-SBD and pLVX-CLTC, pLVX-CLTC(1–494), pLVX-CLTC(1–1073) or pLVX-CLTC-Hub, respectively. After 24 h, the cells were fixed with 1:1 methanol/acetone, and incubated with mouse anti-His (Beyotime) and rabbit anti-HA (Santa Cruz) antibodies for 30 min at 37 °C. After three washes, the cells were incubated with a mixture of FITC-conjugated goat anti-mouse (Boster, Wuhan, China) and Cy3-conjugated goat anti-rabbit secondary antibodies (Beyotime) for 30 min at 37 °C. The nuclei of all treated cells were stained with DAPI, and cover slips were mounted onto a glass slide using 10% glycerol. Confocal images were obtained using a Zeiss LSM 710 scanning confocal microscope.

2.11. Statistical analysis

All data are presented as means ± standard deviation (S.D.). Student's *t*-test and two-way-ANOVA tests were used to compare the data from different treated groups. Statistical significance is indicated as *, $P < 0.05$; **, $P < 0.01$; ***, $P < 0.001$. All statistical analyses and calculations were performed using GraphPad PRISM software (version 7.0 for Windows; GraphPad software Inc.).

3. Results

3.1. Mortalin inhibited PEDV replication

Two isolated PEDV strains: a classical strain JS2008 and a variant strain AH2012/12 (Fig. s1) were used to investigate the effects of mortalin on PEDV replication. Firstly, the expression level of mortalin was down-regulated by transfections with mortalin specific siRNAs (siMor) in Vero cells for 24 h. As shown in Fig. 1A, among the three siRNAs (siMor-1, siMor-2, and siMor-3), the decrease of mortalin protein was most obvious following siMor-1 treatment, when compared with siNC treatment, and no appreciable cytotoxicity could be observed at a concentration of 20 nM of transfected siMor-1 (Fig. 1B). Subsequently, the Vero cells were transfected with siMor-1 and siNC, respectively. After 24 h, the cells were infected with PEDV JS2008 or AH2012/12 at a MOI of 0.1. At 24 hpi, the levels of related proteins and nucleic acid were detected. As shown in Fig. 1C, the expressions of N protein in the siMor-1 treatment groups were significantly increased. Furthermore, the virus yields of JS2008 and AH2012/12 in siMor-1 groups were both significantly higher than those in siNC group (Fig. 1D). These results revealed that the knockdown of mortalin enhanced PEDV replication.

The effects of mortalin overexpression on the replication of PEDV were also detected. As shown in Fig. 1E, the mortalin protein fused His tag was highly expressed in the pLVX-Mor transfection groups. And the levels of N protein in these groups were significant less than those in the pLVX groups. The levels of virus yield titers in supernatants of the pLVX-Mor transfection groups were both obviously less than those of the pLVX transfection groups (Fig. 1F). These results further confirmed that the mortalin inhibited PEDV replication.

3.2. Mortalin interferes with PEDV entry

To analyze the stages of the virus life cycle affected by mortalin, early virus entry was initially assessed by an internalization assay. As shown in Fig. 2A and B, the mRNA and protein levels of mortalin were both significantly decreased in siMor-1-treated cells, and no significant difference ($P > 0.05$) in the amount of adsorbed virus was observed between siMor-1 and siNC-treated cells. However, viral entry in the siMor-1-treated cells was obviously increased when compared with the

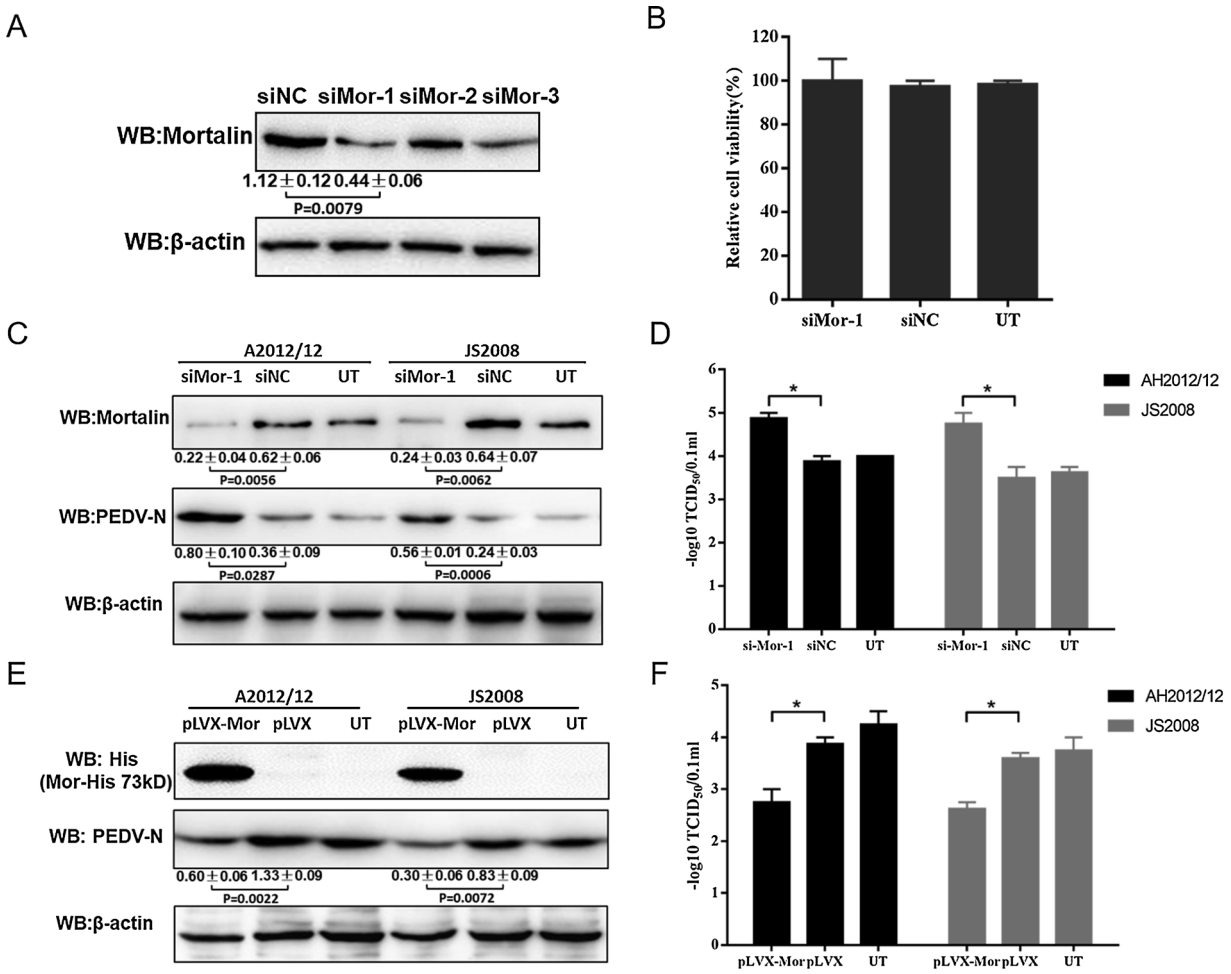

Fig. 1. The effects of mortalin on the replication of PEDV. Three synthesized mortalin siRNAs were transfected into Vero cells for 24 h. The mortalin protein levels (A) and relative cell viabilities of siMor-1 (B) were detected in Vero cells. In order to determine the effects of mortalin on the replication of PEDV, siMor-1 and negative control siNC, pLVX-Mor and pLVX-N1 were transfected into Vero cells for 24 h, respectively. Then all cells were infected with different PEDV strains JS2008 or AH2012/12 (MOI = 0.1). At 24 hpi, the cells were analyzed the expression levels of mortalin and PEDV-N (C and E) by western blotting, and PEDV yields in the supernatant were titrated by the $TCID_{50}$ (D and F). The relative gray values of protein bands according β-actin were marked under the bands. The results are presented as the mean ± SD of data from three independent experiments. *, $P < 0.05$; **, $P < 0.01$; ***, $P < 0.001$. UT: Untreated group.

controls (Fig. 2B), suggesting that mortalin inhibited PEDV entry to the Vero cells. The effects of mortalin on replication and release stages of PEDV life cycle were also investigated. As shown in Fig. 2C and D, the intracellular PEDV genome copy number and the intracellular levels of N protein were almost the same between siMor-1 treated and control cells. And the virus yield titers in the supernatants also showed no significant differences between these two groups at different time points (Fig. 2E).

In addition, we also tested the effects of mortalin overexpression on the PEDV entry by confocal analysis according to the previous description with little modification (Zhang et al., 2018). As shown in Fig. 2F, the number of PEDV virions in mortalin overexpressed (Mor-oe) cells was significantly less than that in normal (Mor-no) cells in the PEDV infected group. And there was no specific virious fluorescence in the control group without virus infection. These results suggested that mortalin inhibited PEDV entry to Vero cells and had no effect on viral replication and release.

3.3. The interaction between mortalin and CLTC

To study the mechanism of mortalin inhibition of PEDV entry. The interaction between mortalin and PEDV S protein was firstly tested, but no interaction was found (data not shown). Subsequently, mortalin antibody was used to precipitate the protein lysate of PEDV-infected Vero cells, and the precipitated product was analyzed by mass spectrometry. As shown in Fig.3A, multiple proteins were detected in the precipitated product, but none of these were virus-related proteins. It was worth noting that CLTC was one detected protein. A previous study revealed that clathrin-mediated endocytosis played a role in PEDV entry into Vero cells (Park et al., 2014), and CLTC is an important part of clathrin. So, we detected the interaction between these two proteins. Firstly, the locations of intracellular mortalin and CLTC were assayed by confocal microscopy with mouse anti-mortalin antibody (Thermo) and rabbit anti-CLTC poly-antibody (ABclonal, Wuhan, China). As shown in Fig.3B, there were co-localizations of mortalin with CLTC in some positions in the cytoplasm of Vero cells. Subsequently, the immunoprecipitation (IP) experiments were performed by expressing the two proteins fusing different tags. A confocal microscopy assay showed considerable co-localization of mortalin with CLTC in cytoplasm of Vero cells (Fig. 3C). The IP assays were performed and revealed that mortalin interacted with CLTC, and vice versa (Fig. 3D).

3.4. Mortalin downregulates CLTC through the proteasome degradation pathway

The relationship of the changes in protein expression levels between mortalin and CLTC was investigated. As shown in Fig. 4A, the protein level of CLTC was significantly decreased when mortalin was

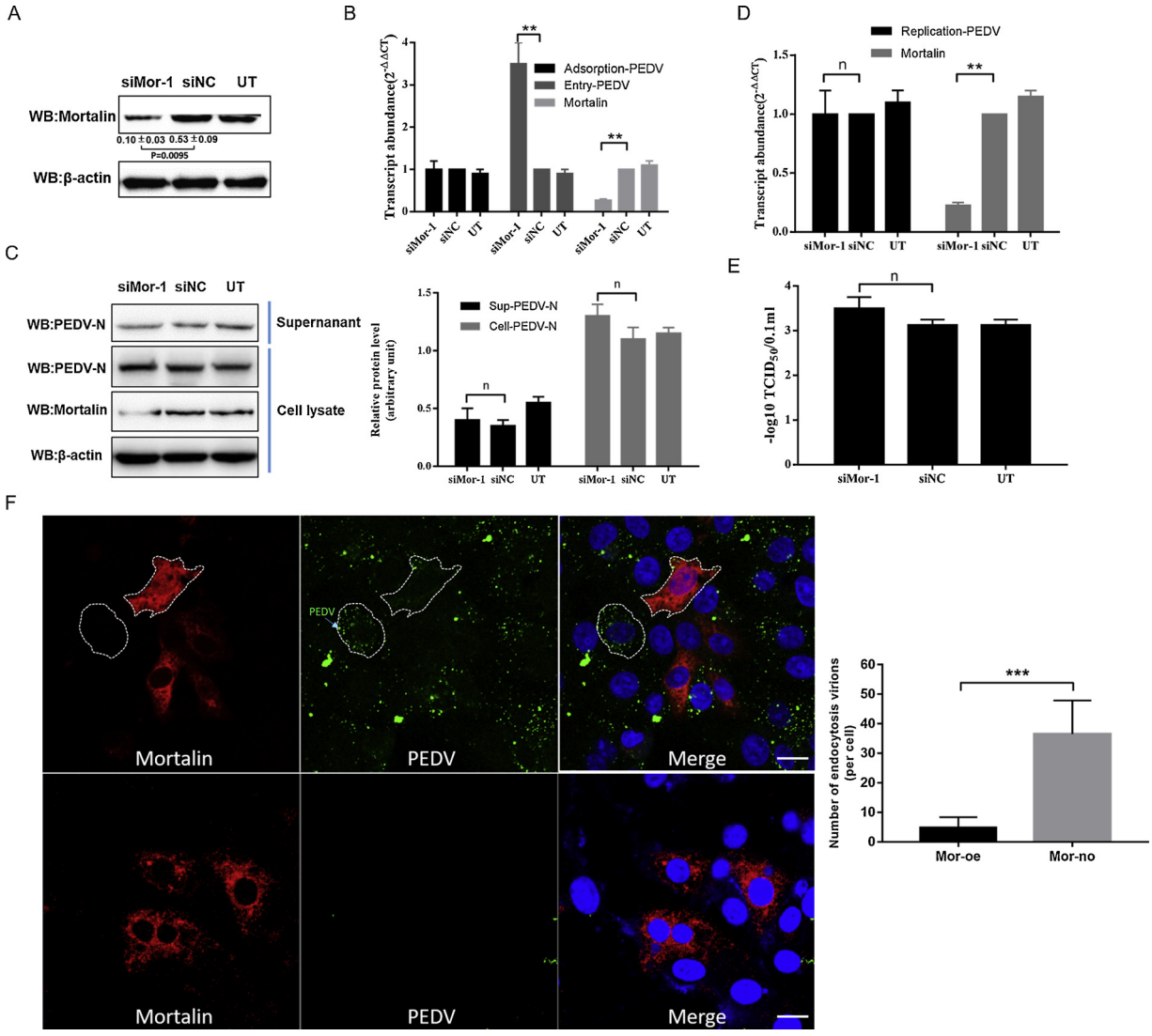

Fig. 2. The effects of mortalin on the key stages of virus replication. Vero cells transfected with siMor-1 or siNC were used to assay effects of mortalin on PEDV adsorption and entry. Then the cell samples were analyzed mortalin protein levels by western blotting (A) and PEDV genome copies by qRT-PCR (B). To determine whether mortalin inhibits PEDV at the replication and release steps. Firstly, cells were incubated with virus, and the cell-free virus particles were removed. Then the cells were transfected with siMor-1 or siNC for 24 h, and the infected cells were analyzed the PEDV N protein levels and the relative gray values according β-actin levels in the supernatant or cell lysates (C), and the intracellular relative quantifications of PEDV copies, mortalin mRNAs (D) and PEDV yields in the supernatants (E). (F) Confocal analysis of the PEDV entry into the mortalin overexpression Vero cells. Vero cells were transfected with pLVX-Mor. After 24 h, the cells were incubated with PEDV (MOI = 10) (up section) or cell culture medium (down section) as control at 4 ˚C for 1 h. Then the cells were washed with ice-cold PBS three times and cultured in fresh serum-free DMEM containing 5 μg/ml trypsin at 37 ˚C for 1 h. Finally, the cells were fixed, and used confocal microscopy to detect PEDV N protein and mortalin. Virions show green fluorescence, and the location of the nucleus shows blue. Scale bar, 20 μm. The column diagram revealed the number of PEDV virions in Mor-oe and Mor-no cells. 20 cells were recorded in each individual experiment. All the results are presented as the mean ± SD of data from three independent experiments. *, $P < 0.05$; **, $P < 0.01$; ***, $P < 0.001$. UT: Untreated group. (For interpretation of the references to colour in this figure legend, the reader is referred to the web version of this article).

transiently overexpressed in cells. In turn, the protein level of CLTC was significantly increased when mortalin expression was disrupted in siMor-1 transfected cells (Fig. 4B). These data revealed that mortalin could downregulate the expression of CLTC.

Several members of Hsp70 family have been reported to facilitate the proteolytic degradation through proteasomal- or lysosomal-dependent pathways (Zhu et al., 2014). The proteasome inhibitor lactacystin and the lysosomal inhibitors pepstatin A/E64D were therefore employed to determine whether mortalin degraded CLTC through the proteasomal- or lysosomal-dependent pathways. As shown in Fig. 4C, following overexpression of mortalin, the protein level of CLTC did not change in the lactacystin pretreatment group, but was significantly reduced in pepstatin A/E64D treatment group. Moreover, in case of mortalin downregulation, the CLTC also did not change in lactacystin pretreatment group, and was significantly increased in pepstatin A/E64D and DMSO pretreatment groups (Fig. 4D). These results revealed that the degradation of CLTC protein was blocked by treatment with the proteasome inhibitor lactacystin, and that mortalin could downregulate CLTC through the protease degradation pathway.

3.5. Mor-SBD interacts with CLTC-Hub, but inhibition of PEDV entry requires complete mortalin protein

To further clarify the regions of interaction between mortalin and CLTC, expression vectors containing truncated versions of these proteins were constructed and expressed (Fig. s2). The CLTC divided into three regions: N-terminal domain and linker (residues 1-494), distal domain (residues 495-1,073) and hub domain (residues 1,074–1,675)

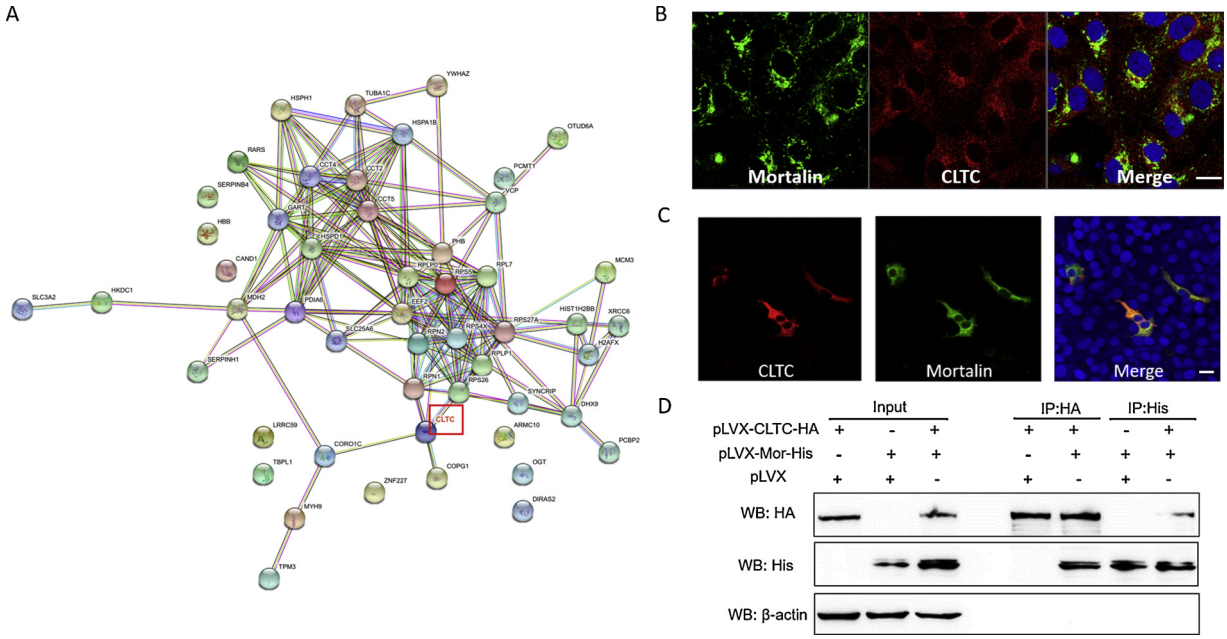

Fig. 3. The interaction between mortalin and CLTC. (A) A network diagram of the detected proteins in the precipitated product by using mortalin antibody. The CLTC protein was labeled with red box. (B) The confocal microscopy assay of mortalin and CLTC in Vero cells. (C) The confocal microscopy assay of mortalin and CLTC with pLVX-Mor-His and pLVX-CLTC-HA transfections. Scale bar, 20 μm. (D) The immunoprecipitation assay of mortalin and CLTC. (For interpretation of the references to colour in this figure legend, the reader is referred to the web version of this article).

(Ybe et al., 1999). Mortalin have two basic domains: the nucleotide-binding domain (NBD; residues 1-384) and the substrate-binding domain (SBD; residues 389-680) (Da and Borges, 2011). A confocal microscopy assay showed that the CLTC(1–494) and CLTC(1–1073) were mainly expressed in the nucleus, without co-localization with full-length mortalin. Whereas, CLTC-Hub showed considerable co-localization with full-length mortalin in the cytoplasm (Fig. 5A). Subsequently, confocal assay revealed that Mor-NBD was expressed in the cytoplasm in an aggregated state, and did not co-localize with full-length CLTC. Whereas, Mor-SBD showed obvious co-localization with full-length CLTC (Fig. 5B). The above results indicated that Mor-SBD and CLTC-Hub were likely to contain the interacting regions. Further IP experiments confirmed that there was interaction between Mor-SBD and CLTC-Hub by using the two proteins fusing different tags through eukaryotic expression vectors (Fig. 5C).

To determine the regions of mortalin responsible for degrading CLTC protein and inhibiting PEDV entry, the different truncated mortalin constructs were overexpressed in Vero cells. As shown in Fig. 5D and E, the amount of CLTC protein decreased significantly and the number of gene copies of PEDV invading cells decreased relatively only

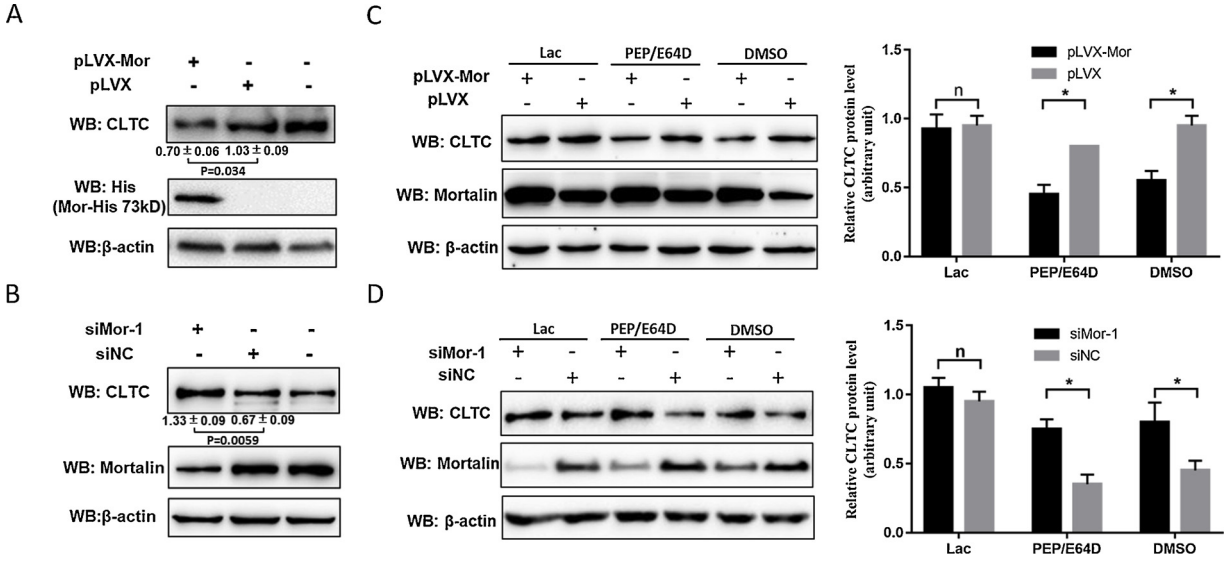

Fig. 4. Mortalin downregulates CLTC through the proteasome degradation pathway. (A) The protein levels of mortalin and CLTC in cells with pLVX-Mor or pLVX transfection. (B) The protein levels of mortalin and CLTC in cells with siMor-1 or siNC transfection. The relative gray values of protein bands according β-actin were marked under the bands. To determine the pathway of mortalin degrade CLTC. Vero cells were treated with proteasome inhibitor lactacystin or lysosomal inhibitors pepstatin A/E64D. After 1 h treatment, the cells were transfected with pLVX-Mor and pLVX-N1 (C) or siMor-1 and siNC (D) for 24 h. Then the expression levels of CLTC and mortalin were detected, and relative expression levels of CLTC according to the grayscale of β-actin in cells were assayed. The results are presented as the mean ± SD of data from three independent experiments. *, $P < 0.05$; **, $P < 0.01$; ***, $P < 0.001$.

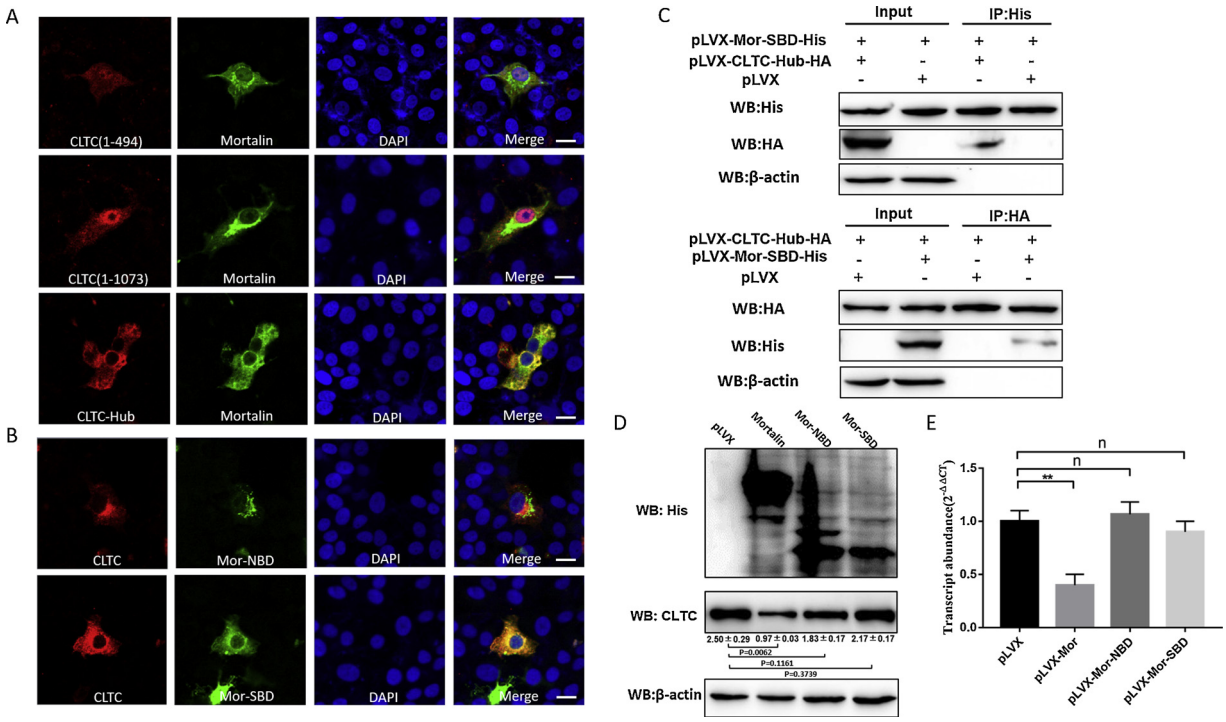

Fig. 5. Determination of the functional regions of mortalin and CLTC. A confocal microscopy assay of the CLTC truncations with full-length mortalin (A) and the mortalin truncations with full-length CLTC (B). The overexpressed proteins were labeled with corresponding tag antibodies. Scale bar, 20 μm. (C) The immunoprecipitation assay of Mor-SBD and CLTC-Hub. To determine the regions of mortalin responsible for degrading CLTC and inhibiting PEDV entry, Vero cells were transfected with the expression vectors of complete mortalin or its truncations. After 24 h, the plates were pre-chilled at 4 °C. Then the cells were incubated with PEDV (MOI = 5)for 1 h at 4 °C, and then were washed and shifted to 37 °C for another 1 h. The protein levels of CLTC (D) and the relative quantifications of PEDV entry numbers (E) in the cells were detected. The relative gray values of protein bands according β-actin were marked under the bands. The results are presented as the mean ± SD of data from three independent experiments. *, $P < 0.05$; **, $P < 0.01$; ***, $P < 0.001$.

when the entire mortalin construct was overexpressed. The above results indicated that for inhibition of PEDV entry, the complete mortalin is needed.

3.6. Mortalin negatively regulates clathrin-mediated endocytosis, and affects PEDV entry further

To further clarify that mortalin inhibits PEDV entry by downregulating clathrin-mediated endocytosis, we traced and visualized the endocytosis of Tf and CT-B whilst changing the expression levels of mortalin in Vero cells. Tf is transported into the cells via the receptor-mediated clathrin-dependent endocytosis pathway. CT-B is internalized and delivered to the Golgi complex through the caveolae-mediated endocytosis pathway (Nichols, 2002). As shown in Fig. 6A, the amount of Tf transported into cells was significantly increased in siMor-treated cells compared with the siNC-treated cells. However, the amount of CT-B transported into cells was not related to the downregulation of mortalin. In mortalin overexpressing cells, the levels of intracellular Tf were significantly lower than those in normal cells, while the levels of intracellular CT-B did not differ between cells irrespective of mortalin overexpression (Fig.6B).

Subsequently, we detected the effects of mortalin and clathrin-mediated endocytosis on PEDV entry by using Vero cells. The results showed that the mortalin downregulation significantly increased the expression of CLTC, but the number of gene copies of PEDV invading Vero cells was not increased under the CPZ treatment, when compared with the siNC transfected groups (Fig. 6C).

In addition, the effects of mortalin and clathrin-mediated endocytosis on PEDV entry by using IPEC-J2 cells were also detected. Firstly, we assayed the effects of mortalin on virus replication in IPEC-J2 cells. As shown in Fig. 7A and B, compared with the control groups, the expressions of N proteins and the virus yields of supernatants were both significantly increased and decreased in the si-pMor and pLVX-pMor transfection groups, respectively. These results revealed that the mortalin also had the ability to inhibit PEDV replication in IPEC-J2 cells. Subsequently, we determined the way of PEDV invading IPEC-J2 cells. The results revealed that PEDV entry into cells followed clathrin-mediated endocytosis independence of caveolae (Fig. 7C and D). Through using CPZ and si-pMor together, we found that the numbers of invading virus in si-pMor treatment groups were not increased under the CPZ treatment, when compared with the siNC transfected groups (Fig. 7E and F). In addition, the numbers of PEDV invading IPEC-J2 cells of si-pMor alone treatment groups were obviously increased compared with the siNC groups. All the above results further indicated that mortalin decreased PEDV entry by downregulating clathrin-mediated endocytosis, both in Vero and IPEC-J2 cells.

3.7. Mortalin interferes with the other virus entry mediated by clathrin

The data from the assays described above indicated that mortalin could degrade CLTC via the proteasomal pathway, and suppress the entry of PEDV by downregulating clathrin-mediated endocytosis further. Whether mortalin could interfere with the entry of other viruses, VSV, TGEV and RV, which also use clathrin-mediated endocytosis to enter host cells (Gutiérrez et al., 2010; Hu et al., 2018; Sun et al., 2005), was also determined. Meanwhile, CSFV, which entry into 3D4/21 cells does not depend on clathrin mediated endocytosis (Zhang et al., 2018), is used as a control. As shown in Fig. 8A, B and C, when compared with the control groups, the genome copy numbers of VSV, TGEV, and RV in the pLVX-Mor and siMor-transfected groups were decreased and increased significantly, respectively. However, there were no significant difference of the CSFV genome copy numbers in pLVX-Mor and siMor-transfected groups compared with the control groups, respectively (Fig. 8D). These results revealed redundant mortalin interfering virus

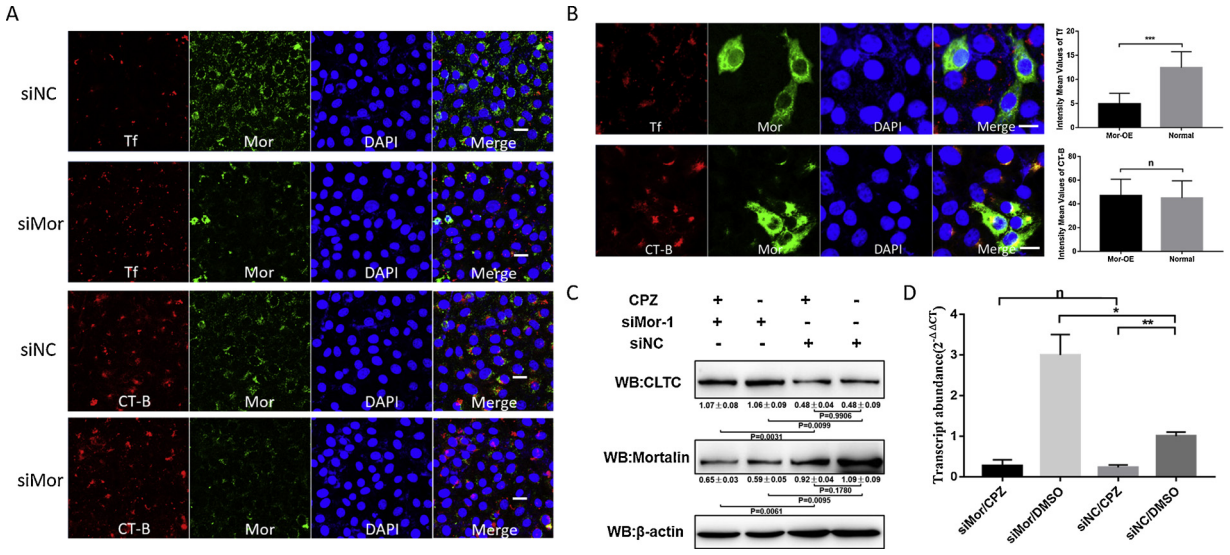

Fig. 6. Mortalin inhibits PEDV entry Vero cel by downregulating clathrin-mediated endocytosis. In order to assay the effect of mortalin on clathrin-mediated endocytosis, siRNA and siNC (A), pLVX-Mor and pLVX-N1 (B) were transfected into cells for 24 h, respectively. Then the cells were pre-chilled at 4 ˚C for 30 min, and incubated with Alexa Fluor 555-Tf or Alexa Fluor 555-CT-B for 30 min at 4 ˚C to synchronize entry, and were then shifted to 37 ˚C for another 15 min. The cells were fixed and analyzed using confocal microscope. The intensity mean values of Tf and CT−B in 20 cells of pLVX-Mor and pLVX-N1 transfected cells were also determined. Scale bar, 20 μm. To determine the effects of mortalin and clathrin-mediated endocytosis on PEDV entry, Vero cells were transfected with siMor-1 or siNC for 24 h, respectively. The clathrin-mediated endocytosis inhibitor: CPZ, was added for 30 min. Then cells were pre-chilled at 4 ˚C, and incubated with PEDV (MOI = 5) for 1 h at 4 ˚C, and were then shifted to 37 ˚C for another 1 h. The protein levels of mortalin and CLTC (C) and the relative quantifications of PEDV entry numbers (D) in the infected cells were assayed. The relative gray values of protein bands according β-actin were marked under the bands. All the results are presented as the mean ± SD of data from three independent experiments. *, P < 0.05; **, P < 0.01; ***, P < 0.001.

entry, which mediated by clathrin.

4. Discussion

Mortalin is localized predominantly in the mitochondria, where it is part of the ATP-dependent mitochondrial protein import machinery, but its presence was also detected in the endoplasmic reticulum, the Golgi network, exosomes, and on the surface of cell(Kaul et al., 2007). There is also evidence that mortalin is involved in the process of viral infection. Mortalin appears to play roles in membrane trafficking and the regulation of viral release, since it interacts with exosomal negative factor (Nef) protein, which is necessary for the secretion of Nef and HIV-1 virus release (Shelton et al., 2012). Mortalin is also involved in replications of dengue virus and Tembusu virus(Kakumani et al., 2016; Liu et al., 2017). In this study, we also found that mortalin acted to inhibit PEDV entry through inducing CLTC degradation by proteasomal pathway, thereby inhibiting the clathrin-mediated endocytosis of PEDV into host cells. When we found that mortalin could restrict PEDV entry,

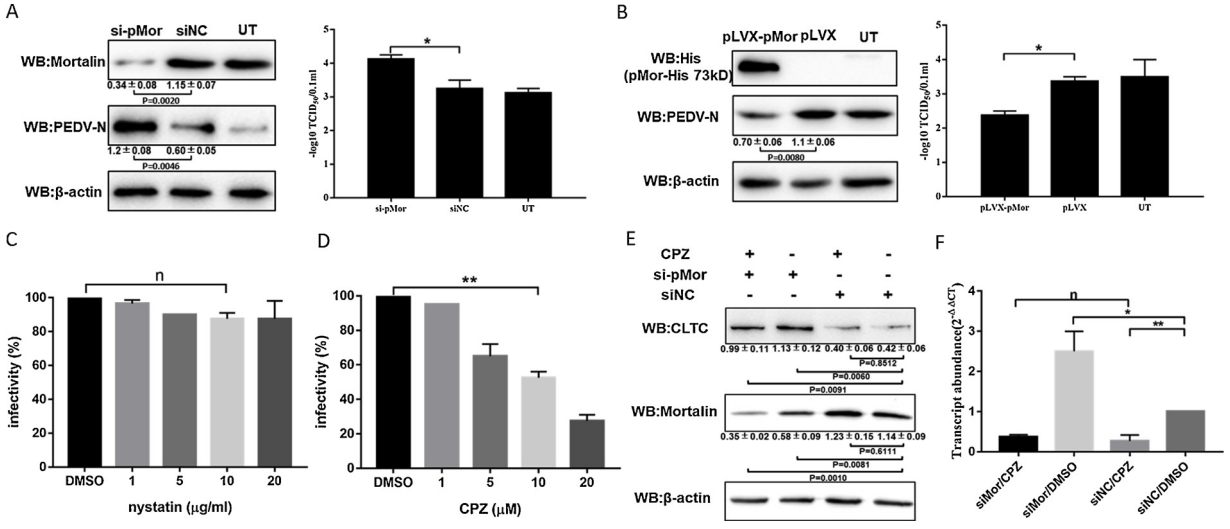

Fig. 7. The effects of mortalin and clathrin-mediated endocytosis on PEDV entry in IPEC-J2 cells. The expression levels of mortalin and PEDV-N, and PEDV yields of the supernatant in the si-pMor (A) and pLVX-pMor (B) transfected groups. To clarify whether PEDV invading IPEC-J2 cells via clathrin-mediated endocytosis (C) or caveolae-mediated endocytosis (D). IPEC-J2 cells were treated with various concentrations of nystatin or CPZ prior to infection, and infected with AH2012/12. PEDV entry was scored by immunocytochemistry at 10 hpi. The relative infectivity was showed as percentages of infected cells to untreated cells. The effects of mortalin and clathrin-mediated endocytosis on PEDV entry were analyzed as above described in Vero cells. The protein levels of mortalin and CLTC (E) and the relative quantifications of PEDV entry numbers (F) in the infected cells were assayed. The relative gray values of protein bands according β-actin were marked under the bands. All the results are presented as the mean ± SD of data from three independent experiments. *, P < 0.05; **, P < 0.01; ***, P < 0.001.

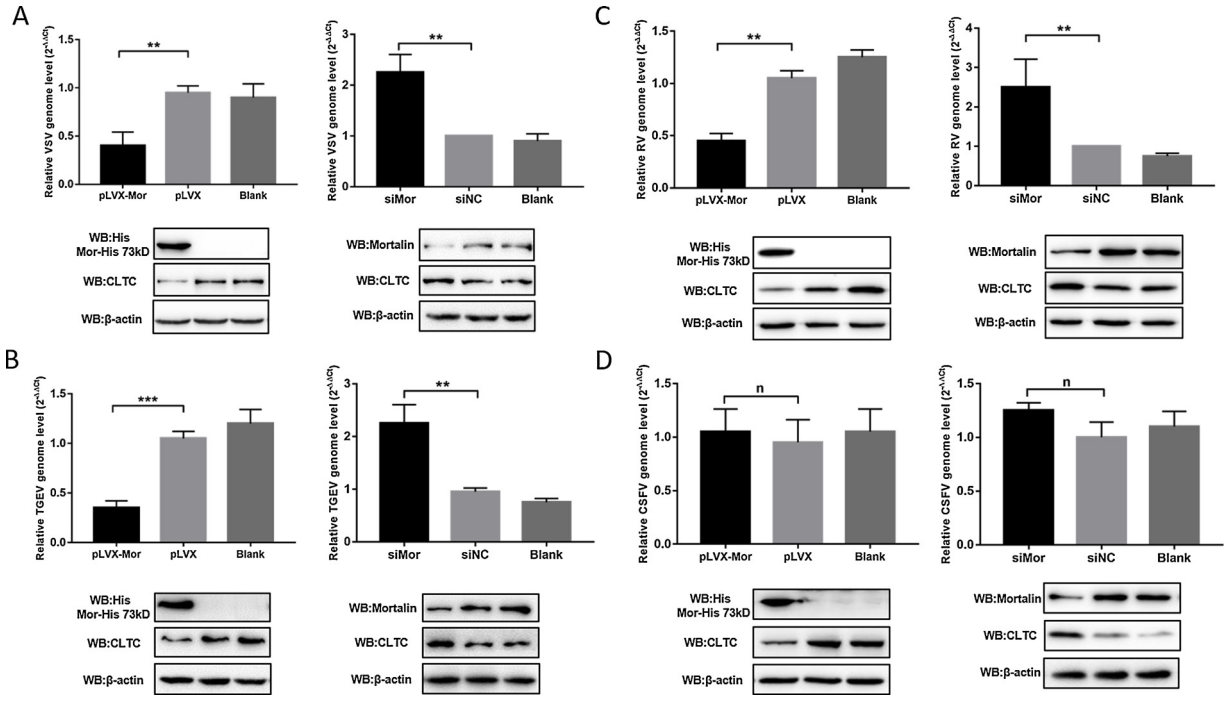

Fig. 8. Effects of mortalin on the clathrin-mediated entry of other viruses. The relative quantifications of virus entry numbers of VSV (A), TGEV (B), RV (C) and CSFV (D), in infected cells with pLVX-Mor or siMor transfection. All the results are presented as the mean ± SD of data from three independent experiments. *, $P < 0.05$; **, $P < 0.01$; ***, $P < 0.001$.

we firstly considered whether mortalin interacted with PEDV S protein. However, the IP assay results showed no interaction between these two proteins (data not shown). Then, we incubated mortalin antibody with lysed PEDV-infected cells and mass spectrometry analysis confirmed the interaction with CLTC protein with a relatively high confidence level. Of course, we cannot exclude the possibility that mortalin also interacts with other proteins of PEDV.

Subsequently, we confirmed the biochemical interaction between mortalin and CLTC, and the regions involved in this interaction were located at the carboxyl terminals of both of the proteins. Moreover, the mortalin can degrade CLTC through the proteasomal pathway. Considering that CLTC is a key component of clathrin triskelion, which plays a role in PEDV entry, it was concluded that mortalin degraded CLTC through the proteasomal pathway, and inhibited the clathrin-mediated endocytosis of PEDV into host cells. Importantly, this host-mounted antiviral mechanism is broadly applicable to other viruses using the same clathrin-mediated endocytic pathway. Through the mechanism study of mortalin inhibiting PEDV replication, we revealed the interaction between mortalin and CLTC, and showed that mortalin could degrade CLTC in host cells through the proteasomal pathway.

Endocytosis is used by cells to compartmentalize components of the plasma membrane and extracellular space into intracellular vesicles that are further distributed into cell compartments. And this process is often used by microbial and viral intruders for infection. Recently, it was shown that mortalin has a role in endocytosis mediated by heparan sulphate proteoglycans (HSPGs) (Wittrup et al., 2010). HSPGs represent a protein family substituted with polysulfated heparan sulphate polysaccharides, and play a role in many virus entry. In this study, we found that mortalin was involved in the process of clathrin-mediated endocytosis, which was also one endocytosis pathway for various viruses' entry to host cells. These results revealed that mortalin could regulate the entry of microorganisms in different ways.

HSP70 s control protein degradation by chaperoning various native polypeptides toward specific proteases. In eukaryotes, HSP70 s can direct ubiquitin E3 ligases onto a polypeptide target to be subsequently degraded by the proteasome (Kettern et al., 2010). HSP70 s have two basic domains: NBD and SBD. The NBD controls the conformational changes in the SBD (Da and Borges, 2011). In this study, we determined that the SBD region of mortalin interacted with the carboxyl terminal of CLTC, but the degradation function of mortalin requires the complete protein. This is probably because the SBD adopts two different conformations, open and closed, which is controlled by the NBD, and these different conformations have different affinities for the substrates.

Previous studies have shown that HSC70, another member of the HSP70 protein family, participated in the disassembly of endocytic clathrin-coated pits. The carboxy-terminal segment of CLTC contains a short region with an amino acid sequence that is preferentially recognized by Hsc70 and mediates clathrin uncoating and release of a free vesicle, primed to fuse with a target membrane (Böcking et al., 2011). In this study, mortalin seems to play an opposite role in down-regulating CLTC protein to inhibit clathrin-mediated endocytosis, when upregulating the expression level of mortalin. Some factors have been determined to alter protein expression levels of mortalin, such as muscle activity and mitochondrial biogenesis (Sadekova et al., 1997). So, a reasonable explanation is that there is a dynamic balance of the CLTC protein level to maintain normal physiological function in normal cells. When cells are stimulated by other factors, the protein levels of mortalin will go to have to change to alter the functions of cells.

5. Conclusion

In this study, we found that mortalin could inhibit the invasion of the viruses which depend on clathrin-mediated endocytosis. We revealed the interaction between mortalin and CLTC, and showed that mortalin could degrade CLTC in host cells through the proteasomal pathway. This study reveals a new function of mortalin in inhibiting endocytosis, and provide a novel strategy for treating PEDV infections.

Declaration of Competing Interest

No potential conflict of interest was reported by the authors.

Acknowledgments

This work was supported by National Key Research and Development Program (2016YFD0500101), the Jiangsu province Natural Sciences Foundation (BK20190003), National Natural Science Foundation of China (31872481 and 31802167), Jiangsu Agricultural Science and Technology Innovation Fund (CX (19) 2020), Six talent peaks in jiangsu province (NY-045) and Jiangsu Provincial Key Construction Laboratory of Probiotics Preparation (JSYSZJ2017004).

Appendix A. Supplementary data

Supplementary material related to this article can be found, in the online version, at doi:https://doi.org/10.1016/j.vetmic.2019.108455.

References

Böcking, T., Aguet, F., Harrison, S.C., Kirchhausen, T., 2011. Single-molecule analysis of a molecular disassemblase reveals the mechanism of Hsc70-driven clathrin uncoating. Nat. Struct. Mol. Biol. 18, 295–301.

Bridgen, A., Kocherhans, R., Tobler, K., Carvajal, A., Ackermann, M., 1998. Further analysis of the genome of porcine epidemic diarrhoea virus. Adv. Exp. Med. Biol. 440, 781–786.

Da, S.K., Borges, J.C., 2011. The molecular chaperone Hsp70 family members function by a bidirectional heterotrophic allosteric mechanism. Protein Pept. Lett. 18.

Duan, E., Wang, D., Fang, L., Ma, J., Luo, J., Chen, H., Li, K., Xiao, S., 2015. Suppression of porcine reproductive and respiratory syndrome virus proliferation by glycyrrhizin. Antiviral Res. 120, 122–125.

Fan, B., Yu, Z., Pang, F., Xu, X., Zhang, B., Guo, R., He, K., Li, B., 2016. Characterization of a pathogenic full-length cDNA clone of a virulent porcine epidemic diarrhea virus strain AH2012/12 in China. Virology 500, 50.

Flachbartova, Z., Kovacech, B., 2013. Mortalin - a multipotent chaperone regulating cellular processes ranging from viral infection to neurodegeneration. Acta Virol. 57, 3–15.

Gutiérrez, M., Isa, P., Sánchezsan, M.C., Pérezvargas, J., Espinosa, R., Arias, C.F., López, S., 2010. Different rotavirus strains enter MA104 cells through different endocytic pathways: the role of clathrin-mediated endocytosis. J. Virol. 84, 9161–9169.

Hiroshi, K., Toru, K., Shunsuke, K., Yuichiro, N., Natsuko, A., Yoshio, M., Katsumi, M., Makoto, T., Minoru, K., 2015. Heat shock protein 70 regulates degradation of the mumps virus phosphoprotein via the ubiquitin-proteasome pathway. J. Virol. 89, 3188–3199.

Hu, W., Zhang, S., Shen, Y., Yang, Q., 2018. Epidermal growth factor receptor is a co-factor for transmissible gastroenteritis virus entry. Virology 521, 33.

Kakumani, P.K., Medigeshi, G.R., Kaur, I., Malhotra, P., Mukherjee, S.K., Bhatnagar, R.K., 2016. Role of human GRP75 in miRNA mediated regulation of dengue virus replication. Gene 586, 7–11.

Kaul, S.C., Deocaris, C.C., Wadhwa, R., 2007. Three faces of mortalin: a housekeeper, guardian and killer. Exp. Gerontol. 42, 263–274.

Kettern, N., Dreiseidler, M., Tawo, R., Hã¶Hfeld, J., 2010. Chaperone-assisted degradation: multiple paths to destruction. Biol. Chem. 391, 481–489.

Kirchhausen, T., Owen, D., Harrison, S.C., 2014. Molecular structure, function, and dynamics of clathrin-mediated membrane traffic. Cold Spring Harb. Perspect. Biol. 6, a016725.

Li, B., Liu, H., He, K., Guo, R., Ni, Y., Du, L., Wen, L., Zhang, X., Yu, Z., Zhou, J., 2013. Complete genome sequence of a recombinant porcine epidemic diarrhea virus strain from Eastern China. Genome Announc. 1, e0010513.

Li, W., Li, H., Liu, Y., Pan, Y., Feng, D., Song, Y., Tang, X., He, Q., 2012. New variants of porcine epidemic diarrhea virus, China, 2011. Emerging Infect. Dis. 18, 1350–1353.

Li, Z., Chen, F., Ye, S., Guo, X., Muhanmmad Memon, A., Wu, M., He, Q., 2016. Comparative proteome analysis of porcine jejunum tissues in response to a virulent strain of porcine epidemic diarrhea virus and its attenuated strain. Viruses 8.

Lin, C.M., Saif, L.J., Marthaler, D., Wang, Q., 2016. Evolution, antigenicity and pathogenicity of global porcine epidemic diarrhea virus strains. Virus Res. 226, 20–39.

Lin, H., Li, B., Chen, L., Ma, Z., He, K., Fan, H., 2017. Differential protein analysis of IPEC-J2 cells infected with porcine epidemic diarrhea virus pandemic and classical strains elucidates the pathogenesis of infection. J. Proteome Res. 16, 2113.

Liu, Q., Huang, X., Zhao, D., Han, K., Liu, Y., Jing, Y., Bi, K., Yin, L., 2017. Identification of heat shock protein A9 on DF-1 cells as a putative receptor for Tembusu virus. Virus Res. 227, 110–114.

Mokranjac, D., Neupert, W., 2009. Thirty years of protein translocation into mitochondria: unexpectedly complex and still puzzling. Biochimica et Biophysica Acta (BBA) - Molecular Cell Research 1793, 33–41.

Nichols, B.J., 2002. A distinct class of endosome mediates clathrin-independent endocytosis to the Golgi complex. Nat. Cell Biol. 4, 374–378.

Park, J.E., Cruz, D.J., Shin, H.J., 2014. Clathrin- and serine proteases-dependent uptake of porcine epidemic diarrhea virus into Vero cells. Virus Res. 191, 21–29.

Pensaert, M.B., de Bouck, P., 1978. A new coronavirus-like particle associated with diarrhea in swine. Arch. Virol. 58, 243–247.

Sadekova, S., Lehnert, S., Chow, T.Y., 1997. Induction of PBP74/mortalin/Grp75, a member of the hsp70 family, by low doses of ionizing radiation: a possible role in induced radioresistance. Int. J. Radiat. Biol. 72, 653–660.

Shelton, M.N., Huang, M.B., Ali, S.A., Powell, M.D., Bond, V.C., 2012. Secretion modification region-derived peptide disrupts HIV-1 Nef's interaction with mortalin and blocks virus and nef exosome release. J. Virol. 86, 406.

Sun, R.Q., Cai, R.J., Chen, Y.Q., Liang, P.S., Chen, D.K., Song, C.X., 2012. Outbreak of porcine epidemic diarrhea in suckling piglets, China. Emerg. Infect. Dis. 18, 161–163.

Sun, X., Yau, V.K., Briggs, B.J., Whittaker, G.R., 2005. Role of clathrin-mediated endocytosis during vesicular stomatitis virus entry into host cells. Virology 338, 53–60.

Wadhwa, R., Yaguchi, T., Hasan, M.K., Mitsui, Y., Reddel, R.R., Kaul, S.C., 2002. Hsp70 family member, mot-2/mthsp70/GRP75, binds to the cytoplasmic sequestration domain of the p53 protein. Exp. Cell Res. 274, 246–253.

Wittrup, A., Zhang, S.H., Svensson, K.J., Kucharzewska, P., Johansson, M.C., Morgelin, M., Belting, M., 2010. Magnetic nanoparticle-based isolation of endocytic vesicles reveals a role of the heat shock protein GRP75 in macromolecular delivery. Proc. Natl. Acad. Sci. U. S. A. 107, 13342–13347.

Xiaozhen, G., Han, H., Fangzhou, C., Zhonghua, L., Shiyi, Y., Shuang, C., Mengjia, Z., Qigai, H., 2016. iTRAQ-based comparative proteomic analysis of Vero cells infected with virulent and CV777 vaccine strain-like strains of porcine epidemic diarrhea virus. J. Proteomics 130, 65–75.

Xuan, H., Xing, D., Wang, D., Zhu, W., Zhao, F., Gong, H., 1984. Study on the Culture of Porcine Epidemic Diarrhea Virus Adapted to Fetal Porcine Intestine Primary Cell Monolayer.

Ybe, J.A., Brodsky, F.M., Hofmann, K., Lin, K., Liu, S.H., Chen, L., Earnest, T.N., Fletterick, R.J., Hwang, P.K., 1999. Clathrin self-assembly is mediated by a tandemly repeated superhelix. Nature 399, 371–375.

Zeng, S., Zhang, H., Ding, Z., Luo, R., An, K., Liu, L., Bi, J., Chen, H., Xiao, S., Fang, L., 2015. Proteome analysis of porcine epidemic diarrhea virus (PEDV)-infected Vero cells. Proteomics 15, 1819–1828.

Zhang, Y.N., Liu, Y.Y., Xiao, F.C., Liu, C.C., Liang, X.D., Chen, J., Zhou, J., Baloch, A.S., Kan, L., Zhou, B., Qiu, H.J., 2018. Rab5, Rab7, and Rab11 are required for caveola-dependent endocytosis of classical swine fever virus in porcine alveolar macrophages. J. Virol. 92.

Zhu, H., Yoshimoto, T., Yamashima, T., 2014. Heat shock protein 70.1 (Hsp70.1) affects neuronal cell fate by regulating lysosomal acid sphingomyelinase. J. Biol. Chem. 289, 27432–27443.